

## Supplementary Information

# Variable densification of reduced graphene oxide foam into multifunctional high-performance graphene paper

Fan Xu <sup>a,b,&</sup>, Ruofan Chen<sup>a,&</sup>, Zaishan Lin<sup>a,b,&</sup>, Xianxian Sun<sup>a,b</sup>, Shasha Wang<sup>a</sup>, Weilong Yin<sup>a,b,\*</sup>,  
Qingyu Peng<sup>a,b,\*</sup> and Yibin Li<sup>a,b,\*</sup>, Xiaodong He<sup>a,b</sup>

<sup>a</sup> Center for Composite Materials and Structures, School of Astronautics, Harbin Institute of Technology, Harbin 150080, P. R. China.

<sup>b</sup> Shenzhen STRONG Advanced Materials Research Institute Co.,LTD, Shenzhen 518000, P. R. China.

\*Corresponding authors. Email: [liyibin@hit.edu.cn](mailto:liyibin@hit.edu.cn), [pengqingyu@hit.edu.cn](mailto:pengqingyu@hit.edu.cn), [ywl@hit.edu.cn](mailto:ywl@hit.edu.cn)

&These authors equally contribute the manuscript.

## **Supplementary Information:**

### **Electrical conductivity measurement technique.**

**Figure S1.** The schematic illustration of the electrical conductivity test method (a) and the voltammetry curves (b).

**Figure S2.** The optical photo of TAGP.

**Figure S3.** Survey scan XPS spectra.

**Figure S4.** Raman spectra of TAGP, the density varies from  $0.32\text{g/cm}^3$  to  $1.53\text{g/cm}^3$ .

### **Tear resistance test method.**

**Figure S5.** The schematic illustration of the tear resistance test sample (a) and test method (b).

**Figure S6.** The optical photos of tearing process.

**Figure S7.** The curve of tearing with loading and time.

**Figure S8.** The different bending angle of GP.

**Figure S9.** The sample of after tearing test: (a) Our TAGP; (b) Panasonic graphene paper.

### **Thermal conductivity test method.**

**Figure S10.** Schematic illustration of: (a) the self-heating experimental setup, and (b) the testing measurements of the thermal conductivity.

**Figure S11.** The microstructure of graphene layer. SEM images of graphene oxide (a) and thermal annealing graphene (b); TEM images of graphene oxide (c) and thermal annealing graphene (d). Scale bars:  $2\ \mu\text{m}$  in (a) and (b);  $500\ \text{nm}$  in (c) and (d);  $2\ \text{nm}$  in (c inset) and (d inset).

### **The calculation method of EMI SE.**

**Figure S12.** Comparison the performances of GA and TAGA: (a) electrical conductivity; (b) EMI SE.

**Figure S13.** Comparison of average  $SE_t$ ,  $SE_a$  and  $SE_r$  of TAGA and TAGP ( $80\ \mu\text{m}$ ) with the same quality.

### Electrical conductivity measurement technique.

The electrochemical workstation (PARSTAT4000) was used to measure the electrical conductivity by two-probe method. The simple circuit diagram is shown as Figure S1a. The length, width and thickness of test samples are 70 mm, 5 mm and 0.1 mm, respectively. The graphene paper was connected by two electrodes, and the voltammetry was used to test the resistance of graphene paper. Figure S1b is the voltammetry curves of graphene paper. The electrical conductivity equation can be written as:

$$R = \frac{U}{I}$$

$$R = \rho \frac{L}{S}$$

$$\sigma = \frac{1}{\rho} = \frac{L}{Rs}$$

where L, S are the length and cross-section area of the sample, and R, U, I are the resistance, voltage and current, and  $\rho$ ,  $\sigma$ , are the electrical resistivity and electrical conductivity, respectively.

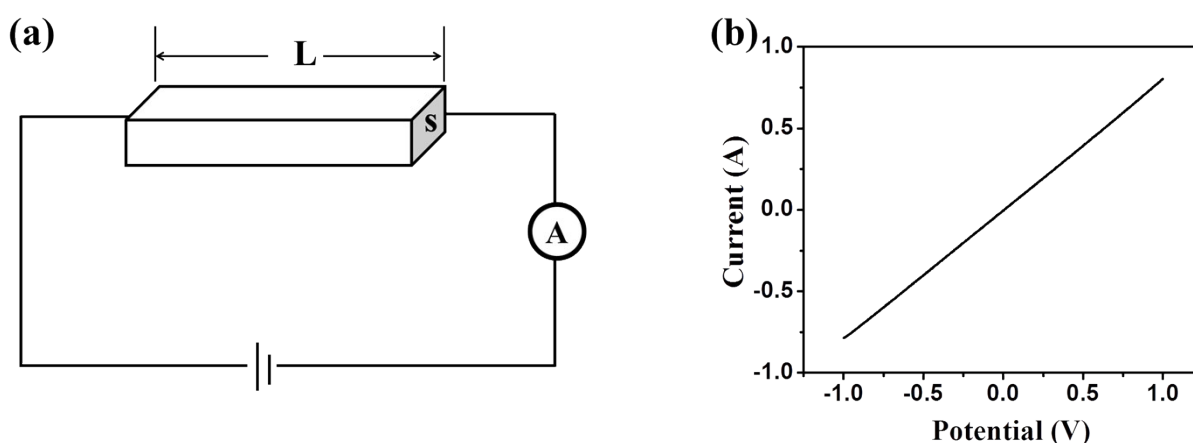


**Figure S1.** The schematic illustration of the electrical conductivity test method (a) and the voltammetry curves (b).

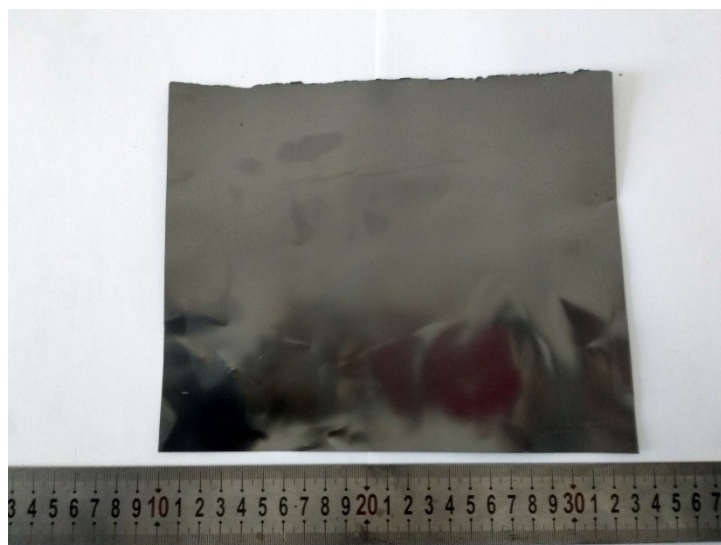


**Figure S2.** The optical photo of TAGP.

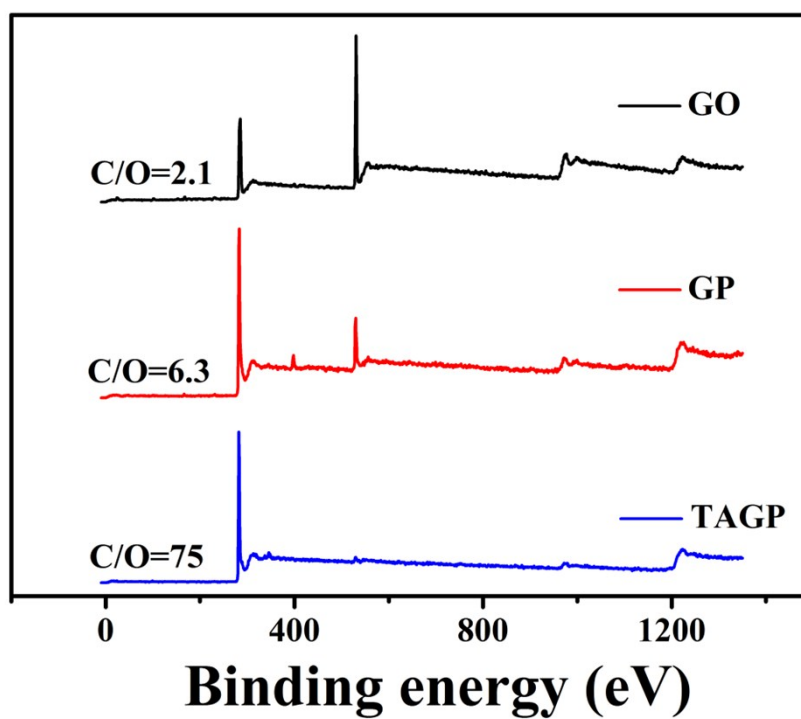


**Figure S3.** Survey scan XPS spectra.

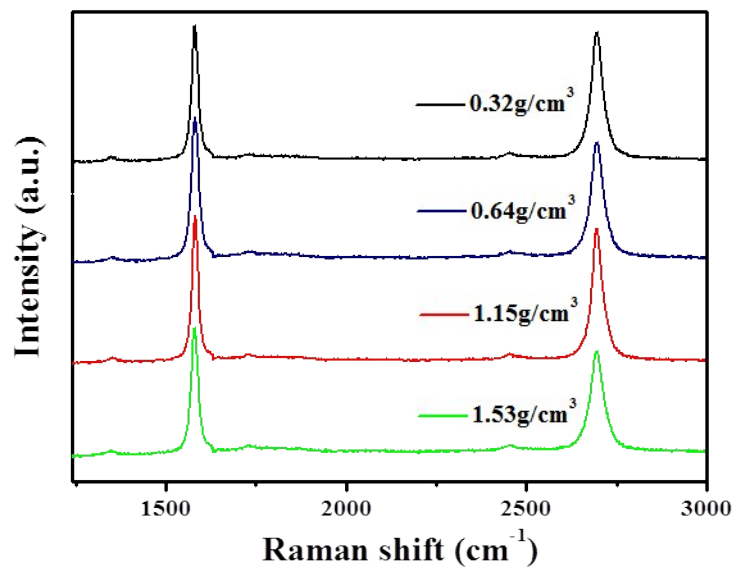


**Figure S4.** Raman spectra of TAGP, the density varies from  $0.32\text{g/cm}^3$  to  $1.53\text{g/cm}^3$ .

### **Tear resistance test method:**

Tear resistance is tested by the trousers-type tear method, the schematic illustration as Figure S5. The graphene paper was cut into pieces, the geometry of sample was 0.05 mm thickness, 10 mm width and 30 mm length, then, the sample was cut a gap to the middle along the length.(Figure S5a) The sample was clamped on stretcher as Figure S5b. The optical photos of tearing process were shown in Figure S6.

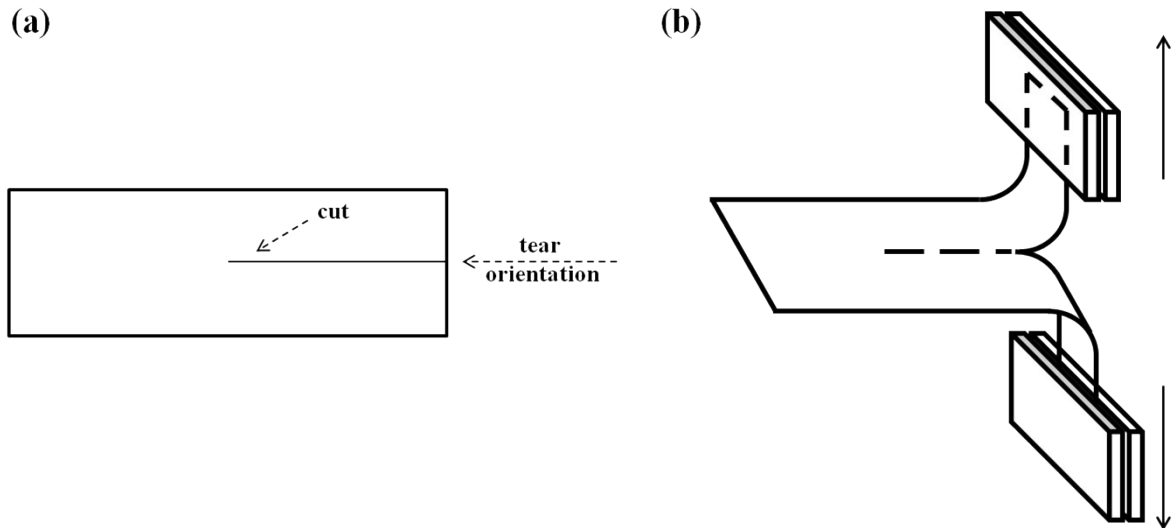


**Figure S5.** The schematic illustration of the tear resistance test sample (a) and test method (b).

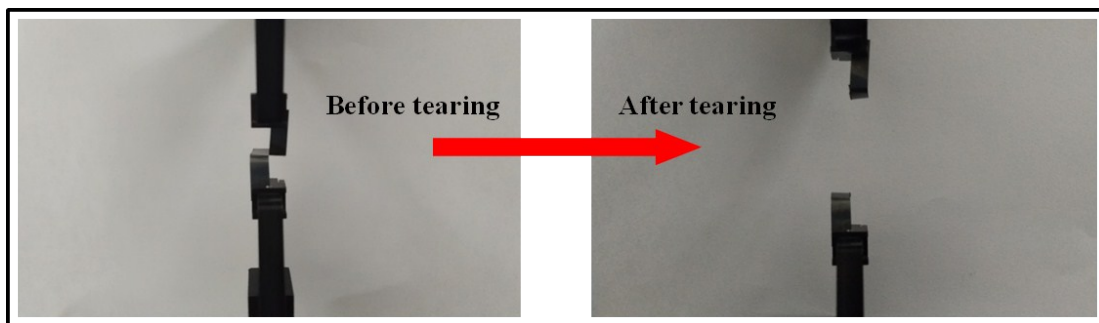


**Figure S6.** The optical photos of tearing process.

We can get a curve with time and tearing force. As shown in Figure S7, tearing process is including three stages, first stage (marked as zone “I” ) is the incipient stage, second stage is the stabilized stage (marked as zone “II” ) and third stage is the finished stage (marked as zone “III” ). Usually, the average value of loading in zone II is considered as “tearing force”. The tear resistance is tearing force to the thickness of sample. The calculation as:

$$\sigma = F/d$$

$\sigma$  is the tear resistance,  $F$  is the tearing force,  $d$  is the thickness of sample. The unit is  $\text{N mm}^{-1}$ .

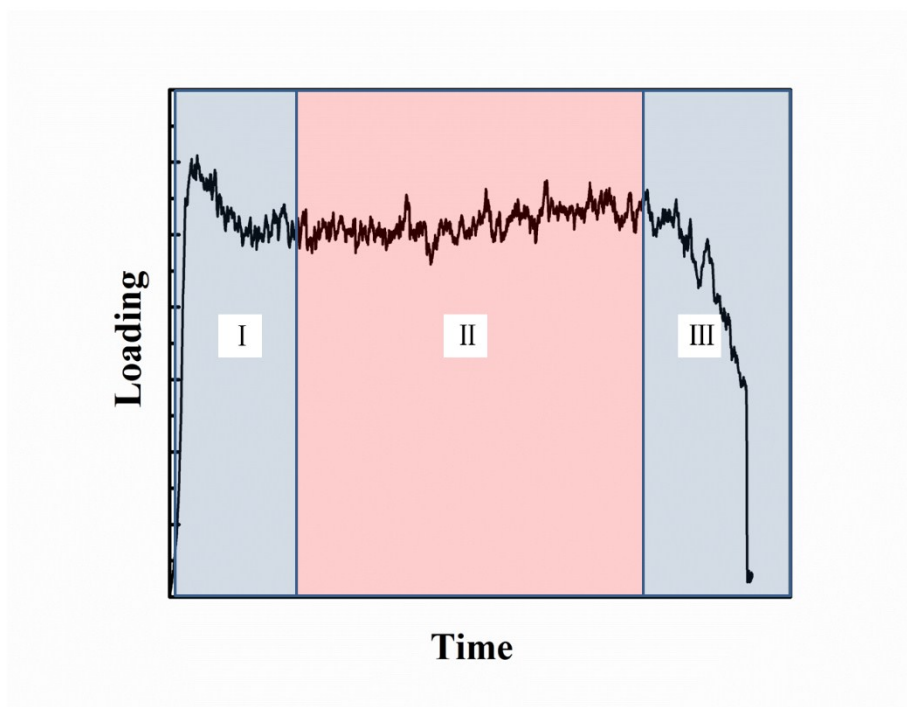


**Figure S7.** The curve of tearing with loading and time.

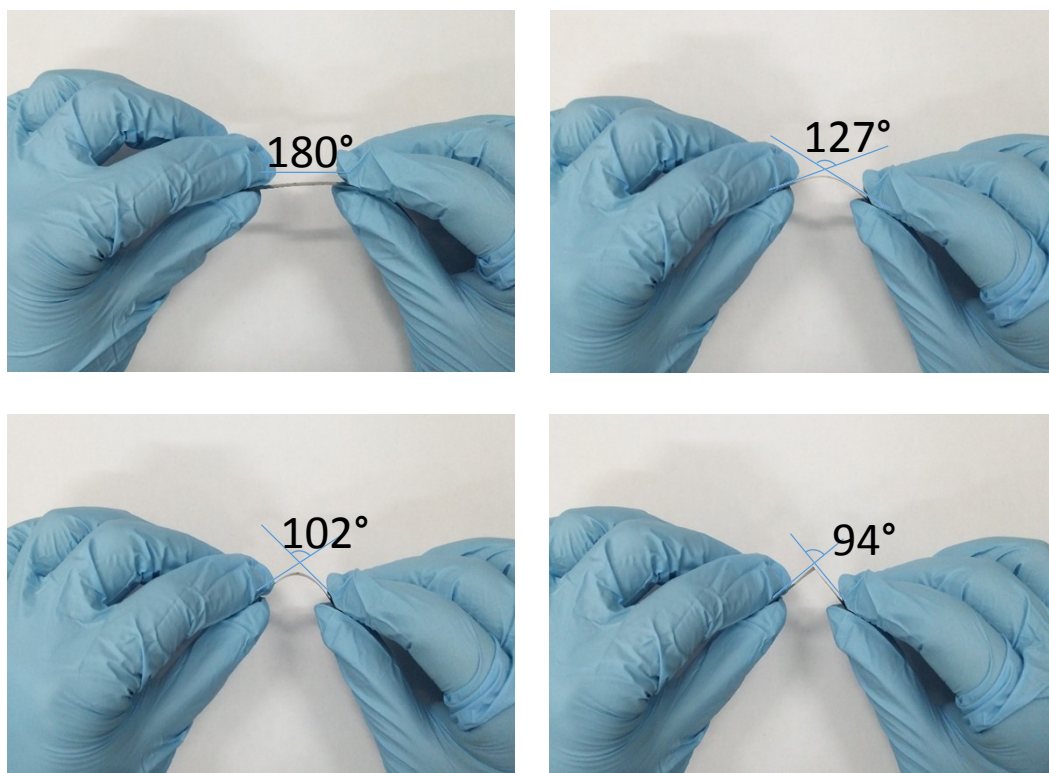


**Figure S8.** The different bending angle of GP.

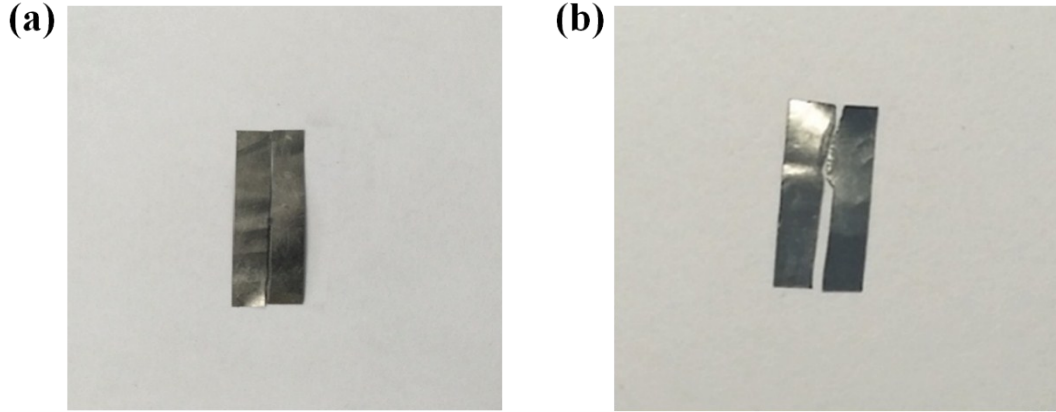


**Figure S9.** The sample of after tearing test: (a) Our TAGP; (b) Panasonic graphene paper.

### **Thermal conductivity test method:**

The Schematic illustration of the testing device has been shown in Figure S10. The graphene papers were cut into slices of 2 mm wide and 70 mm long, we can assume that the volumetric heat generation due to Joule heating,

$$q = UI/2LA_c$$

where  $L$ ,  $A_c$  are the half-length and cross-section area of the slice, and  $U$ ,  $I$ , are the voltage and current, respectively. The one-dimensional steady-state heat transfer equation can be written as:

$$-kA_c \frac{dT^2}{dx^2} + hp(T - T_0) = \frac{UI}{2L}$$

Where  $p$ ,  $k$  and  $h$  are the cross-section perimeter, thermal conductivity and the effective radiation heat transfer coefficient, respectively. When the temperature increase is small, the heat loss to the surroundings attributed to convection and radiation can be neglected. Then we can rewrite the equation as follows:



$$k \frac{d^2 T}{dx^2} + q = 0$$

$$T_x = T_0 + \frac{q}{2k} (L^2 - x^2)$$

The thermal conductivity of the graphene slice can be obtained by:

$$k = \frac{UIL}{4A_c (T_M - T_0)}$$

The thermal conductivity ( $k$ ) was obtained via the slope from the linear fitting  $T_M - T_0$  and  $UI$ .

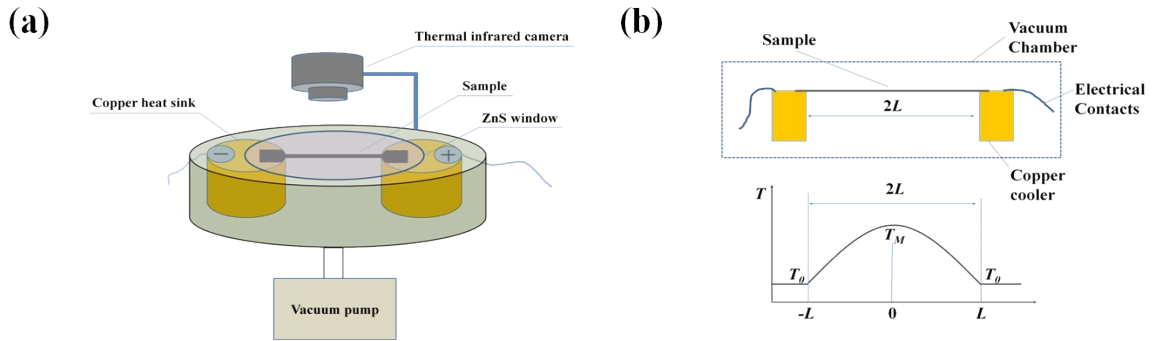


**Figure S10.** (a) Schematic illustration of the self-heating experimental setup; (b) Schematic illustration of the testing measurements of the thermal conductivity.

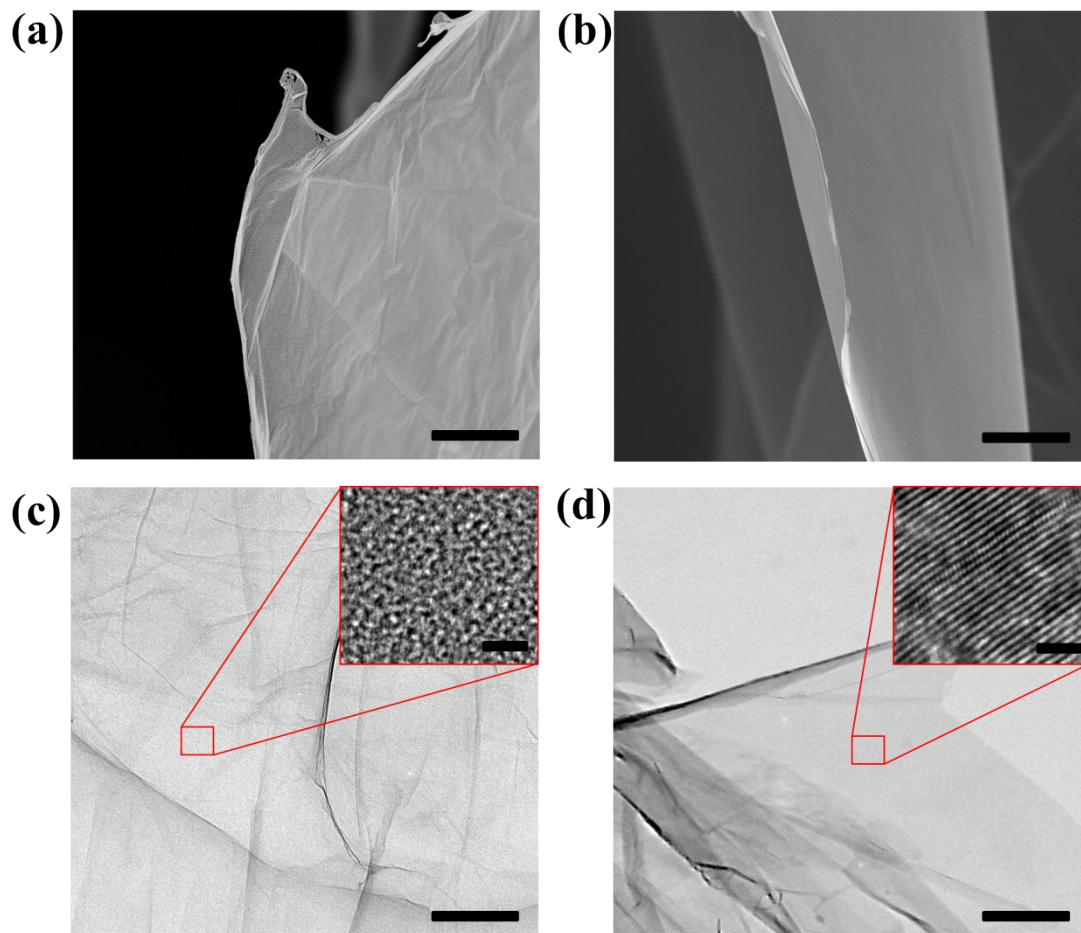


**Figure S11.** The microstructure of graphene layer. SEM images of graphene oxide (a) and thermal annealing graphene (b); TEM images of graphene oxide (c) and thermal annealing graphene (d). Scale bars: 2  $\mu\text{m}$  in (a) and (b); 500 nm in (c) and (d); 2 nm in (c inset) and (d inset).

### The calculation method of EMI SE:

The EMI shielding effectiveness was measured by using an Agilent N5234A vector network analyzer in the frequency range of 2-40 GHz. The sample were cut to fit the waveguide sample for measurement. As shown in table S1, the different measurement frequency needs different waveguide tube, and suitable samples. The thickness of GP is 50  $\mu\text{m}$ , and the thickness of TAGPs are 50  $\mu\text{m}$  and 80  $\mu\text{m}$  with 1.85  $\text{g}/\text{cm}^3$ . Particularly, we have tested the same quality of the TAGPs with different density, the thickness of 0.32  $\text{g}/\text{cm}^3$ , 0.64  $\text{g}/\text{cm}^3$ , 1.15  $\text{g}/\text{cm}^3$ , 1.53  $\text{g}/\text{cm}^3$  and 1.85  $\text{g}/\text{cm}^3$  is

460  $\mu\text{m}$ , 230  $\mu\text{m}$ , 130  $\mu\text{m}$ , 100  $\mu\text{m}$  and 80  $\mu\text{m}$ , respectively.

**Table S1** The corresponding frequency and sample size (length  $\times$  width)

Frequency (GHz)	Size(mm $\times$ mm)
1.7-2.6	109.22 $\times$ 54.61
2.6-3.95	72.14 $\times$ 34.04
3.95-5.85	47.55 $\times$ 22.15
5.85-8.2	34.85 $\times$ 15.80
8.2-12.4	22.86 $\times$ 10.16
12.4-18	15.80 $\times$ 7.90
18-26.5	10.67 $\times$ 4.32
26.5-40	7.11 $\times$ 3.56

Through the vector network analyzer, we can measure  $S_{11}$ ,  $S_{22}$ ,  $S_{21}$ ,  $S_{12}$  four parameters, then calculate R, T as follow:

$$R = |S_{11}|^2 = |S_{22}|^2$$

$$T = |S_{21}|^2 = |S_{12}|^2$$

$$A + R + T = 1$$

Where absorbance (A), reflectance (R) and Transmittance (T) were determined on the basis of the measured S parameters.

The effective absorbance can be expressed as

$$A_{eff} = (1 - R - T)/(1 - R)$$

The total EMI SE ( $SE_{Total}$ ) of a shielding material is the sum of absorption( $SE_A$ ), reflection( $SE_R$ ) and multiple reflection ( $SE_M$ ). The  $SE_{Total}$  is defined as the logarithmic ratio of incident power ( $P_i$ ) to transmitted power ( $P_t$ ).

$$SE_{total} = 10\log(P_i / P_t) = SE_R + SE_A + SE_M$$

When  $SE_{Total} > 15$  dB,  $SE_M$  can be neglected, and it is usually assumed that

$$SE_{Total} \approx SE_R + SE_A$$

$$SE_R = -10\log(1 - R)$$

$$SE_A = -10\log(T/1 - R)$$

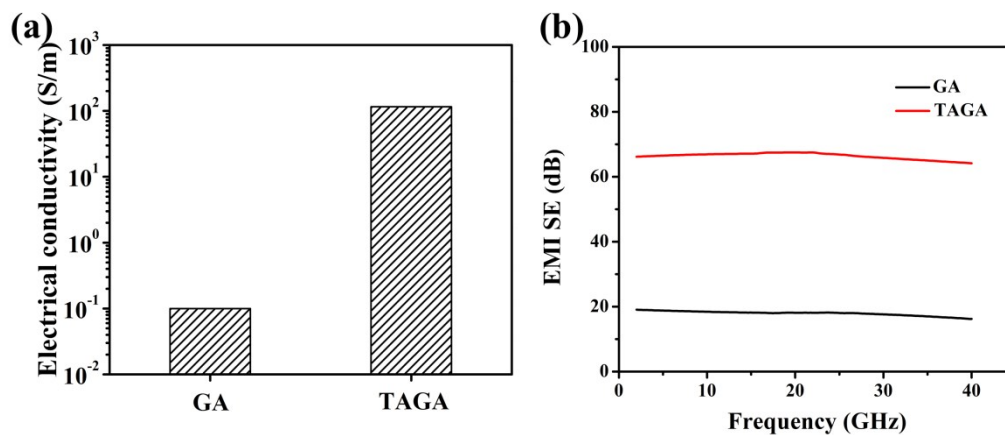


**Figure S12.** Comparison the performances of GA and TAGA: (a) electrical conductivity; (b) EMI SE.

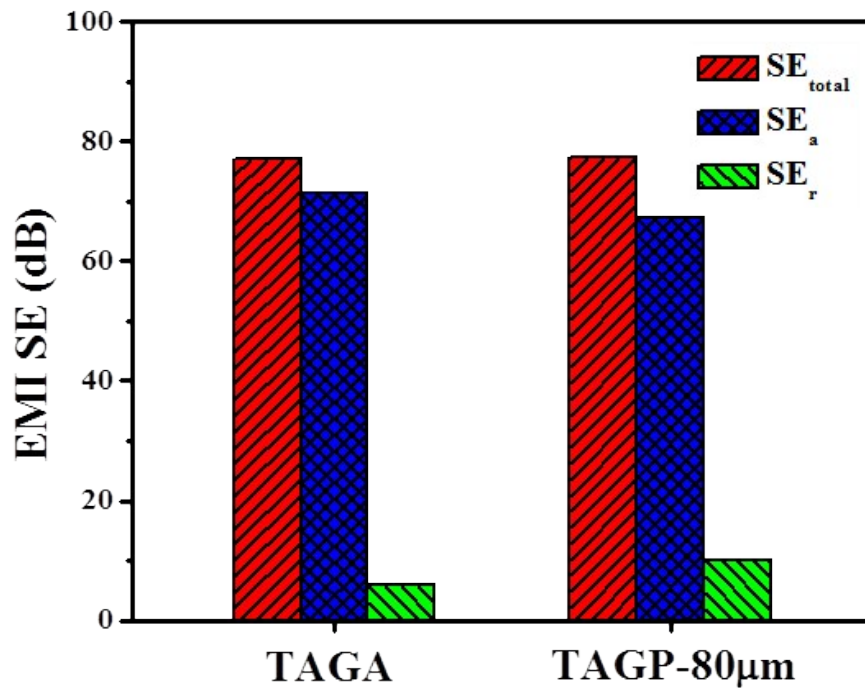


**Figure S13.** Comparison of average  $SE_t$ ,  $SE_a$  and  $SE_r$  of TAGA and TAGP (80 µm) with the same quality.